



Published in final edited form as:

Biomaterials. 2009 February ; 30(6): 1143–1149. doi:10.1016/j.biomaterials.2008.11.001.

Acellularization of embryoid bodies via physical disruption methods

Alyssa V. Ngangan^a and Todd C. McDevitt^{a,b,*}

^aThe Wallace H. Coulter Department of Biomedical Engineering, Georgia Institute of Technology and Emory University, 313 Ferst Drive, Suite 2102, Atlanta, GA 30332-0535, USA

^bThe Parker H. Petit Institute for Bioengineering and Bioscience, Georgia Institute of Technology, Atlanta, GA, USA

Abstract

Embryonic stem cells (ESCs) are capable of differentiating into all somatic cell types and have therefore attracted significant interest for use in tissue repair and regeneration therapies. Transplanted ESCs can not only integrate into compromised tissues, but can also stimulate endogenous regeneration via secreted factors. In this study, several acellularization protocols were applied to spheroids of differentiating ESCs, termed embryoid bodies (EBs), to develop a potential route to deliver ESC-derived molecules, independent of cells, to damaged tissues. The objective of this study was to physically disrupt EBs via lyophilization or freeze-thaw cycling, and in combination with DNase treatment, determine the efficacy of acellularization based upon cell viability, DNA removal, and protein retention. Mechanical disruption and DNase treatment of EBs efficiently inhibited viability and removed DNA while retaining protein content to produce an acellular EB matrix. The EB-derived acellular matrices permitted attachment and repopulation of the constructs by 3T3 fibroblasts *in vitro*. Overall, these studies demonstrate that effective mechanical means to acellularize EBs may be used in order to further elucidate the composition and function of embryonic extracellular matrices and serve as novel naturally-derived scaffolds for tissue repair and regeneration.

Keywords

Acellularization; Decellularization; Embryoid bodies; Extracellular matrix; Embryonic stem cells; Differentiation

1. Introduction

Embryonic stem cells (ESCs) have the ability to self-renew and differentiate into multiple cell types of the three germ layers (ectoderm, endoderm, and mesoderm). The pluripotency of ESCs makes them an attractive cell source for regenerative cell therapies to treat a broad array of degenerative diseases and traumatic injuries. ESCs and ESC-derived cells have been transplanted into areas of damaged tissue where resultant cell repopulation and recovery of tissue function have been demonstrated [1–6]. Use of ESCs as a delivery vehicle for trophic factors has also been shown to be effective in stimulating regeneration of a number of different tissues [7,8]. Notably, Fraidenna et al. discovered that ESCs rescued embryonic lethal

© 2008 Elsevier Ltd. All rights reserved.

*Correspondence to: Todd C. McDevitt, The Wallace H. Coulter Department of Biomedical Engineering, 313 Ferst Drive, Suite 2102, Atlanta, GA 30332-0535, USA. Tel.: +1 404 385 6647; fax: +1 404 894 4243. E-mail address: todd.mcdevitt@bme.gatech.edu (T.C. McDevitt).

knockouts via secretion of soluble molecules, and not by cellular repopulation [7]. Hence, ESC-derived molecular cues are capable of stimulating tissue remodeling events by inducing morphogenesis of endogenous cell populations.

Acellularization techniques provide a means to extract cells from tissues, thereby isolating the extracellular matrix (ECM) components. The ECM provides a natural scaffold for structural support of tissues and harbors a complex assembly of biochemical cues comprised of proteins, glycosylaminoglycans, proteoglycans, and growth factors. Numerous tissues from various sources have been acellularized in order to create scaffolds for tissue regeneration, including small intestinal submucosa (SIS) [9], esophagus [10], bladder [11], cardiac valve [12,13], dermis [14,15], nerve [16], placenta [17], and pericardium [18]. Several techniques have been developed to acellularize tissues via treatment with various solutions and/or mechanical disruption methods. Solution-based approaches typically combine chemical treatments, such as detergents [16,19–22], alkaline or acid solutions [23,24], and hyper- or hypo-tonic solutions [22], as well as enzymatic digests, including trypsin, endonucleases, and ectonucleases [25, 26]. While chemical and enzymatic methods effectively remove cellular content, they usually require multiple incubation and rinsing steps to ensure thorough removal or inactivation of acellularization reagents and may unintentionally remove desirable ECM components. On the other hand, mechanical methods of acellularization, including repeated freeze-thawing, sonication, or other physical means of disrupting cells' plasma membranes [27,28], provide a direct and rapid means of acellularizing tissues, but used alone, such methods are not capable of completely removing cellular material. Thus, a combination of physical and chemical/enzymatic methods is needed to successfully acellularize tissues.

The primary criterion for acellularization is efficient inhibition of tissue viability coupled with preservation of native ECM composition and structure. Lyophilization is a mechanical acellularization method that utilizes freeze-drying to permeabilize cell membranes, as a result of intracellular ice formation during the freezing process, and subsequent removal of water molecules. A number of tissues and acellular matrices have been lyophilized prior to therapeutic application, including bovine pericardium [29,30], bone matrix [31], amniotic membrane [32], and cardiac valves [12]. Freeze-thaw cycling is another mechanical acellularization technique which entails repeated snap-freezing of tissue by submersion in liquid nitrogen followed by thawing at room temperature in a buffered aqueous solution. Multiple freeze-thaw cycles have been utilized to render a variety of tissues acellular, including peripheral nerve grafts [27,33], meniscal tissue [34], embryonic chick knee [35], and human dermis [36]. The aforementioned studies demonstrated that mechanical cell disruption is a mild acellularization treatment that preserves tissue components for successive tissue repair, but thus far, such methods have only been used to acellularize somatic tissues in a homeostatic state.

ESCs are commonly induced to differentiate *in vitro* by forming 3-dimensional cell spheroids, termed embryoid bodies (EBs), which recapitulate many of the molecular and cellular morphogenic events that occur during the normal pre-gastrulation stages of embryological development [37–40]. Previously, our lab demonstrated that acellular matrices could be derived from EBs using solvent extraction methods in combination with DNase treatment [41,42]. The objective of the present study was to examine the effectiveness of two separate mechanical methods, lyophilization and repetitive freeze-thaw cycles, as alternative means to efficiently acellularize matrices produced by differentiating ESCs within EBs. Acellularization was assessed based upon quantitative assays of cell viability, DNA content, and protein content compared to untreated EBs, in addition to histological analysis of acellular EB matrix structure and exogenous cell repopulation of EB-derived matrices. These studies establish methods by which mechanical disruption techniques effectively acellularize EBs to produce acellular matrices capable of supporting cell attachment and adhesion. Naturally-derived matrices from

EBs provide a scaffolding material for future investigations of endogenous tissue repair and regeneration, in addition to elucidating mechanisms by which ESCs promote healing and morphogenesis via the production of unique combinations of factors constituting an embryonic microenvironment.

2. Methods and materials

2.1. ESC culture and differentiation

D3 murine embryonic stem cells were cultured on 0.1% gelatin-coated plates in complete media consisting of Dulbecco's Modified Eagle Medium (DMEM, Mediatech) supplemented with 15% fetal bovine serum (FBS, Hyclone), 2 mM L-glutamine, 1X non-essential amino acids, 100 U/mL penicillin, 100 µg/mL streptomycin, 0.25 µg/mL amphotericin, 0.1 mM β-mercaptoethanol, and 10³ U/mL leukemia inhibitory factor (LIF, Chemicon). To initiate ESC differentiation, embryoid bodies (EBs) were formed from a single-cell suspension of 4 × 10⁶ cells in 10 mL differentiation media (complete media without LIF). EBs were cultured in 100 mm Petri dishes on a rotary orbital shaker (Lab-Line Lab Rotator, Barnstead) held constant at 40 ± 2 rpm [43]. EBs were re-fed with fresh media every 2 days by collecting individual plates of EBs via gravity-induced sedimentation in 15 mL conical tubes, aspirating the old media, and replacing with fresh differentiation media before transferring the EBs back to 100 mm Petri dishes. Rotaries were calibrated every day to ensure constant speed throughout the course of EB culture.

2.2. Acellularization of EBs

After 4, 7, or 10 days of rotary orbital suspension culture, EBs were harvested, rinsed in phosphate-buffered saline (PBS) prior to acellularization treatments, counted, and divided into aliquots of approximately 2 × 10³ EBs per sample. To acellularize via lyophilization, EB samples in 1.5 mL microcentrifuge tubes were rinsed twice with 1 mL PBS and frozen in 1 mL dI H₂O at -80°C overnight. Frozen samples were placed in the lyophilizer (Labconco) overnight and then removed for further processing. Freeze-thawed acellular samples were produced by aspirating PBS, immersing the entire tube with EBs into liquid nitrogen, and allowing the liquid nitrogen to boil off. Once the liquid nitrogen was boiled off, 1 mL PBS was added to thaw the EBs while rotating the sample for 5 min (LabQuake Rotisserie) at room temperature. EBs were then centrifuged for 2 min at 18,000 rcf at room temperature. This process of freeze-thawing was performed 1, 3, or 5 times for each sample to determine the optimal number of cycles. For comparison purposes, chemical acellularization was performed, as previously described, by treating the EB samples with 1% Triton X-100 for 30 min while rotating [41]. Following Triton treatment, samples were centrifuged for 2 min at 18,000 rcf at room temperature and rinsed 3 times with PBS. For DNase treatment, subsequent to mechanical and chemical per-meabilization steps, samples were treated with 0.5 mL of 1 mg/mL DNase for 15 min while rotating, centrifuged for 2 min at 18,000 rcf at room temperature, and rinsed 3 times with 1 mL PBS.

2.3. Scanning electron microscopy (SEM)

Samples not dried via lyophilization (i.e. hydrated samples) were fixed in 2.5% glutaraldehyde in deionized (dI) H₂O for 1 h while rotating. Samples were rinsed 3 times in dI H₂O and rotated in 4% osmium tetroxide in dI H₂O for 1 h at room temperature. After 3 rinses in dI H₂O, samples were placed in acetone and dehydrated using an E3000 series critical point dryer (Quorum Technologies). Liquid CO₂ was allowed to permeate the samples for 1 h and passed through the CO₂ critical point (31.5 °C, 1100 psi). Subsequently, dried samples were mounted on stubs with carbon tape and sputter-coated with gold for 120 s using a Polaron Sputter Coater SC 7640 (Quorum Technologies). Scanning electron microscopy images were taken using a Hitachi S-800 FE-SEM with a 10 kV acceleration voltage.

2.4. Histology

Histological samples were fixed for 30 min in 10% formalin while rotating, washed 3 times in PBS, and embedded in Histogel®. The embedded samples were paraffin-processed and sectioned into 5 µm sections. Prior to staining, slides were de-paraffinized in a Leica Autostainer XL. Hemotoxylin and eosin (H&E) staining was performed using a Leica Autostainer XL, and slides were incubated with Hoechst dye (nuclear stain, 10 µg/mL) for 5 min. Slides were mounted with coverslips using either Cytoseal™ 60 for H&E (Richard-Allan Scientific) or Gel/Mount™ with anti-fading agents for Hoechst (Biomedica Corp.). Brightfield and fluorescent images were captured using a Nikon 80i Upright Microscope and a SPOT Flex camera (15.2 64Mp Shifting Pixel, Diagnostic Instruments) in conjunction with SPOT Advanced v.4.5 (Diagnostic Instruments) software.

2.5. Cell viability

Relative cell viability was analyzed using 10% alamarBlue (Biosource) in serum-free complete media without LIF. Acellular samples and untreated viable EBs were incubated for 2 h in 5% CO₂ at 37 °C, after which 25 µL aliquots were taken from the incubated samples, and fluorescence measurements were taken (ex: 545 nm, em: 590 nm) using a SpectraMax M2e plate reader. Relative measures of viability were determined by comparing the acellular samples to the starting population of untreated viable EBs (viability = 1) and the alamarBlue solution alone (no cells; viability = 0).

2.6. DNA analysis

Viable and acellular EBs were solubilized by rotating samples at room temperature for 24 h in 6_M guanidine hydrochloride in order to assess DNA content. DNA content was quantified using the Quant-iT™ PicoGreen® dsDNA Assay kit (Molecular Probes); a 1:5 volumetric ratio of solubilized sample to a solution of 1X TE buffer and 0.5X PicoGreen dye was used. The fluorescence reading (ex: 485 nm and em: 528 nm) was taken on a SpectraMax M2e plate reader, and the absolute amount of DNA (mg/mL) was quantified against a lambda DNA standard curve (0 mg/mL–5 mg/mL). The amount of DNA present following DNase treatment was compared to untreated EBs.

2.7. Protein analysis

Total protein content was analyzed using a bicinchoninic acid (BCA) assay kit (Pierce). A 1:1 dilution of 6_M guanidine hydrochloride solubilized sample (described above) in dI H₂O was used, and 25 µL of sample was incubated with BCA solution for 30 min. Absorbance readings were taken at 562 nm using the aforementioned plate reader. The absorbance readings of the solubilized samples were compared against a standard curve (0 µg/mL–2000 µg/mL) generated using bovine serum albumin (BSA) in order to calculate absolute protein concentrations.

2.8. Cell seeding

NIH-3T3 fibroblasts were cultured to 80% confluence on tissue culture-treated 100 mm dishes in growth media containing DMEM supplemented with 10% bovine growth serum (BGS, Hyclone), 4_{mM} L-glutamine, 100 U/mL penicillin, and 100 µg/mL streptomycin. Three hours prior to seeding, 3T3s were treated with mitomycin-C (10 µ_M in serum-free growth media) to inhibit cell proliferation for assessment of cell invasion into the acellular matrix. Following acellularization treatments, acellular EB matrices were frozen at –80 °C in 1 mL dI H₂O overnight and freeze-dried. Fibroblasts were trypsinized and seeded onto the lyophilized acellular matrices at a density of 10⁶ cells/mL by placing the matrices into 1 mL of 3T3 single-cell suspension and allowing them to rotate. After 3 h of seeding in suspension, seeded matrices were gently spun down for 1 min at 200 rcf, washed 3 times in PBS, and transferred to 48-well tissue culture plates with 500 µL of 3T3 growth media. The seeded matrices were re-fed every

2 days for up to 4 days, at which point, seeded matrices were rinsed with PBS and processed for histology as previously described.

2.9. Statistics

All statistical analyses were performed using Systat software (version 12). Viability comparisons across multiple experimental groups were conducted using a one-way analysis of variance (ANOVA) followed by post-hoc Tukey analysis to determine significant differences ($p < 0.05$) between the different groups. Comparisons within DNA and protein content results were performed using a two-way ANOVA with significance assessed using post-hoc Tukey analysis ($p < 0.05$).

3. Results

Overall results exhibited efficient acellularization of EBs using mechanical permeabilization with DNase treatment. Initial studies were performed varying the number of freeze-thaw cycles (1, 3, or 5) and examined on the basis of inhibition of cell viability and retention of total protein content. Using EBs differentiated for 7 days (Fig. 1A), investigation of the number of freeze-thaw cycles indicated that 3 cycles was efficient at removing DNA while retaining protein in the final product (Supplementary data, Fig. 1). Successive studies were performed to assess acellularization efficiency on EBs at various stages of differentiation. Both mechanical methods, lyophilization and 3 freeze-thaw cycles, independent of EB differentiation time, significantly inhibited cell viability ($p = 5.57 \times 10^{-6}$) compared to untreated EBs; retention of total protein among EBs at different stages of differentiation after acellularization, however, was not significantly different (Supplementary data, Fig. 2) from untreated EBs. Day 4 EBs generally exhibit relatively low gene expression of ECM molecules and growth factors, whereas a variety of ECM and growth factor gene expression levels begin to increase by day 7 of differentiation and continue to increase by 10 days (Nair, Ngangan, and McDevitt, unpublished results, in preparation). Thus, based on the earliest time point at which ECM molecules are clearly present within EBs, day 7 EBs were used for all subsequent studies.

3.1. Morphology and ultrastructure analysis

The two different mechanical disruption methods attempted yielded acellular products with very different macroscopic properties. Lyophilized EBs were maintained as distinct EBs with a “cottonball, powder-like” morphology (Fig. 1B and C) while freeze-thawed EBs (FT) produced a single amorphous mass with a “gel-like” appearance (Fig. 1D and E). Handling the lyophilized EBs was similar to managing a dry powder with static interaction, while the congealed, freeze-thawed EB matrix could be manipulated by collecting the entire mass using a spatula. EB matrices treated with DNase, both lyophilized (L + D) and freeze-thawed (FT + D), formed a more compact pellet compared to FT matrices and could be gently manipulated using a pair of tweezers.

Compared to untreated EBs (Fig. 2A and D), the lyophilized matrices appeared relatively smooth and largely porous (Fig. 2B and E), whereas FT matrices consisted of a non-porous, dense particulate material, due to compaction from the centrifugation steps performed during acellularization (Fig. 2C and F). After DNase treatment and centrifugation retrieval of the material, L + D samples were less porous and more closely resembled the structure of the FT ± D samples (Supplementary data, Fig. 3). However, subsequent freeze-drying of lyophilized or FT samples after DNase treatment resulted in more “powder-like” and porous materials based upon SEM analysis (data not shown). These results indicate that the sequence of the processing steps performed strongly affects the structural properties of the acellular matrices in their final forms.

3.2. Histological analysis

Several notable differences in the histological appearance of lyophilized and FT EBs were also apparent. As indicated initially by SEM, lyophilized EBs were maintained as separate EBs that appeared similar in size and morphology to untreated EBs (Fig. 3A and B), while repeated freeze-thawing caused individual EBs to agglomerate and form a cohesive mass of indistinguishable EBs (Fig. 3C), much like Triton- or SDS-treated EBs [41,42]. Mechanical acellularization methods alone did not remove cellular content, since nuclei were present within the resulting EB matrices (Fig. 3A–C; 3A–C insets), compared to Triton-treated samples which lacked distinct nuclei [41]. The more intense Hoechst staining of lyophilized and FT EBs (Fig. 3B,C insets) was most likely due to condensation of the cell nuclei by both treatments. Treatment with DNase after physical permeabilization methods resulted in acellular matrices without discrete nuclei by hemotoxylin staining (Fig. 3E and F) and little to no detectable Hoechst staining for DNA content (Fig. 3E and F insets), demonstrating the effectiveness of DNase treatment. In contrast, DNase alone was not able to effectively permeate untreated EBs (Fig. 3D; 3D inset) to disrupt and remove DNA. Thus, the mechanical acellularization protocols produced matrices with different compositions and varying extents of cell DNA removal.

3.3. Quantitative analysis

A multi-parametric set of analyses was performed to quantitatively assess differences in cell viability, DNA removal, and residual protein content resulting from the different acellularization treatments starting with 2×10^3 EBs per sample. Based on a relative scale, the viability of the cells (Fig. 4A) was significantly inhibited (value < 0.05) by both mechanical acellularization methods ($p < 0.001$), as well as by Triton detergent treatment ($p < 0.001$), compared to viable, untreated EBs (value = 1), but no significant differences between the different permeabilization treatments were observed. Each of the relative values approached the lower sensitivity range of the assay, indicating successful devitalization of cells by each of the independent methods prior to DNase treatment. The freeze-thaw method of permeabilization allowed the most efficient removal of DNA (removing $75.02 \pm 8.06\%$ DNA), exhibited by the significant difference ($p = 1.35 \times 10^{-5}$) in residual DNA between FT and FT + D samples (Fig. 4B). DNA content remaining in L + D and T + D samples were not significantly reduced compared to lyophilized ($p = 0.763$) and Triton-treated ($p = 0.336$) samples, respectively. Prior to DNase treatment, overall protein content was not significantly reduced between mechanical permeabilization methods compared to untreated EBs, whereas, Triton per-meabilization significantly decreased the amount of protein ($p = 0.001$) compared to untreated EBs (Fig. 4C). With DNase treatment, mechanically permeabilized products exhibited similar protein content to chemically permeabilized samples, indicating that residual protein removal was a result of the subsequent incubation and wash steps following DNase treatment. Overall acellularization using mechanical disruption techniques with DNase was capable of producing acellular EB matrices with slightly increased protein content compared to acellularized EBs using detergent solvent extraction methods.

3.4. Cell repopulation of acellular EB matrices

Fibroblast (NIH-3T3) cell attachment to and repopulation of the resulting acellular EB matrices was examined 4 days after seeding the cells. As previously demonstrated, negligible Hoechst staining was observed in the unseeded acellularized matrices following DNase treatment (Fig. 3E and F). Exogenously added fibroblasts were easily distinguished from any residual ESC nuclei based on the larger size of the fibroblast nuclei (Fig. 5A and E), roughly twice that of ESCs. Auto-fluorescence of the acellular matrix under the FITC channel (green) was used to distinguish the acellular matrix from the exogenously seeded cells (Fig. 5B and F). Fibroblasts seeded onto lyophilized matrices attached primarily to the surface of individual lyophilized EBs, but did not appear to invade the acellular matrices; similarly, FT matrices without DNase

treatment did not exhibit much infiltration by 3T3 fibroblasts (Supplementary data, Fig. 4). Although the bulk of fibroblasts were distributed throughout the exterior layers of the acellular matrices with DNase treatment, many cells were found within the acellular matrices as well (Fig. 5C,D,G,H). Thus, L + D and FT + D treatments of EBs both permitted fibroblast attachment, adhesion, and repopulation of the acellular matrices.

4. Discussion

The aim of this study was to develop mechanical acellularization methods to isolate extracellular matrices produced by ESCs undergoing differentiation as EBs. The use of mechanical disruption techniques was investigated as an alternative approach to previously reported solvent extraction methods capable of acellularizing EBs [41,42]. EBs were deemed acellular based on inhibition of cell viability, removal of DNA, and retention of protein content, thereby producing an EB-derived matrix capable of supporting exogenous cell adhesion and survival. Isolation of acellular matrices from EBs enables further characterization of the complex assembly of ECM molecules dynamically produced by ESCs as they differentiate. These acellular matrices may be utilized as inductive or instructive biological scaffolds in order to determine the functional effects of ESC-derived ECM biomolecules on somatic and progenitor cell phenotypes in the context of the repair and regeneration of acute and chronically wounded adult tissues.

In most cases thus far when stem cells have been applied to regenerate tissues, the lasting effects typically observed do not include stable engraftment and maturation of the transplanted stem cells. This phenomenon suggests that transplanted cells exert a transient impact on tissue morphogenic processes, such as secretion of trophic factors locally that modulate endogenous cell repair of the injured or degenerative tissue site. In fact, recent studies have demonstrated the ability of factors secreted by ESCs to rescue lethal knockout phenotypes and enhance somatic cell survival [7,44–46]. Morphogenic molecules, such as growth factors and cytokines, secreted by ESCs could be non-covalently associated with elements of the ECM produced by the cells. Such molecules could thus be retained within the acellular matrix of EBs using mechanical disruption techniques, such as lyophilization and repeated freeze-thaw cycles, as described in the present study.

Acellularization of tissues has yielded several naturally-derived matrices that are currently being applied to treat an array of different clinical wounds and injuries. Almost all existing acellularized matrices originate from adult tissue sources, which typically exhibit significantly less regenerative capacity than embryonic tissues actively undergoing development. Within the developing embryo, paracrine factors, particularly morphogens and mitogens, are secreted in latent and bioactive forms into the ECM of the local microenvironment to direct subsequent cell differentiation and tissue morphogenesis. As EBs differentiate, a similar cadre of morphogens and mitogens are produced within EBs; thus, using EBs as the starting tissue source for acellularization provides a unique opportunity to harness complex assemblies of molecules directly from EBs mimicking the process of embryogenesis *in vitro*. By acellularizing EBs at various stages of differentiation using different types and combinations of permeabilization and extraction methods, the biomolecules associated with the differentiation of EBs that are secreted into the ECM can be effectively harnessed and subsequently analyzed.

The development of acellular matrices derived from stem cells provides an alternative regenerative medicine approach to the use of stem cells in addition to direct transplantation and engineering of tissues from stem cell sources. Matrices derived from stem cells provide a natural substrate for cell adhesion and a vehicle to present instructive, morphogenic cues to cells capable of repopulating the scaffold material. Acellular EB matrices may provide a potent

combination of morphogenic factors produced locally by ESCs undergoing differentiation within the unique 3D microenvironment of EBs. In the future, acellular EB matrices could possibly be tailored for specific tissue applications by directing ESCs within EBs to differentiate towards specific cell phenotypes, which in turn could yield “tissue-specific” extracellular matrices from a single pluripotent cell source. The results of this study demonstrate that mechanical acellularization of EBs is a route to directly obtain ESC-derived ECM molecules for potential regenerative medicine therapies.

5. Conclusions

The ability to harness ESC-produced molecules to stimulate tissue morphogenesis independent of the cells themselves is an approach in regenerative medicine. Acellularizing embryoid bodies using mechanical methods provides a means to analyze secreted molecules by ESCs in a matrix formulation that can be further tested *in vitro* to assess effects on migration, proliferation, and differentiation of a variety of different progenitor and somatic cell types. The composition of biomolecules present in the EB matrix is unique to differentiating embryonic stem cells mimicking early stages of embryogenesis. Thus, the molecular cues produced during EB differentiation and harbored within the extracellular matrix could have broad applications in tissue regeneration strategies.

Supplementary Material

Refer to Web version on PubMed Central for supplementary material.

Acknowledgements

Dr. Priya Ramaswami and Rekha Nair provided critical review of the manuscript. Financial support was provided by funding from the Georgia Tech/Emory Center for the Engineering of Living Tissues (GTEC, NSF EEC-9731463) and the NIH (R21 EB007316). AN is supported by an NIH Training Grant (GM008433).

Appendix

Supplementary data

Refer to Web version on PubMed Central for supplementary material.

Appendix

Figures with essential colour discrimination. Parts of Fig. 3 and Fig 5 in this article are difficult to interpret in black and white. The full colour images can be found in the online version, at doi:10.1016/j.biomaterials.2008.11.001.

References

1. Cui L, Jiang J, Wei L, Zhou X, Fraser JL, Snider BJ, et al. Transplantation of embryonic stem cells improves nerve repair and functional recovery after severe sciatic nerve axotomy in rats. *Stem Cells* 2008;26(5):1356–1365. [PubMed: 18308951]
2. Hodgson DM, Behfar A, Zingman LV, Kane GC, Perez-Terzic C, Alekseev AE, et al. Stable benefit of embryonic stem cell therapy in myocardial infarction. *Am J Physiol Heart Circ Physiol* 2004;287(2):H471–H479. [PubMed: 15277190]
3. Kimura H, Yoshikawa M, Matsuda R, Toriumi H, Nishimura F, Hirabayashi H, et al. Transplantation of embryonic stem cell-derived neural stem cells for spinal cord injury in adult mice. *Neurol Res* 2005;27(8):812–819. [PubMed: 16354541]

4. Kolossov E, Bostani T, Roell W, Breitbach M, Pillekamp F, Nygren JM, et al. Engraftment of engineered ES cell-derived cardiomyocytes but not BM cells restores contractile function to the infarcted myocardium. *J Exp Med* 2006;203(10):2315–2327. [PubMed: 16954371]
5. von Unge M, Dirckx JJ, Olivius NP. Embryonic stem cells enhance the healing of tympanic membrane perforations. *Int J Pediatr Otorhinolaryngol* 2003;67(3):215–219. [PubMed: 12633919]
6. Wei L, Cui L, Snider BJ, Rivkin M, Yu SS, Lee CS, et al. Transplantation of embryonic stem cells overexpressing Bcl-2 promotes functional recovery after transient cerebral ischemia. *Neurobiol Dis* 2005;19(1–2):183–193. [PubMed: 15837573]
7. Fraidenraich D, Stillwell E, Romero E, Wilkes D, Manova K, Basson CT, et al. Rescue of cardiac defects in id knockout embryos by injection of embryonic stem cells. *Science* 2004;306(5694):247–252. [PubMed: 15472070]
8. Guttinger M, Fedele D, Koch P, Padrun V, Pralong WF, Brustle O, et al. Suppression of kindled seizures by paracrine adenosine release from stem cell-derived brain implants. *Epilepsia* 2005;46(8):1162–1169. [PubMed: 16060924]
9. Badylak SF, Record R, Lindberg K, Hodde J, Park K. Small intestinal submucosa: a substrate for in vitro cell growth. *J Biomater Sci Polym Ed* 1998;9(8):863–878. [PubMed: 9724899]
10. Bhrany AD, Beckstead BL, Lang TC, Farwell DG, Giachelli CM, Ratner BD. Development of an esophagus acellular matrix tissue scaffold. *Tissue Eng* 2006;12(2):319–330. [PubMed: 16548690]
11. Bolland F, Korossis S, Wilshaw SP, Ingham E, Fisher J, Kearney JN, et al. Development and characterisation of a full-thickness acellular porcine bladder matrix for tissue engineering. *Biomaterials* 2007;28(6):1061–1070. [PubMed: 17092557]
12. Curtil A, Pegg DE, Wilson A. Freeze drying of cardiac valves in preparation for cellular repopulation. *Cryobiology* 1997;34(1):13–22. [PubMed: 9028913]
13. Kasimir MT, Rieder E, Seebacher G, Silberhumer G, Wolner E, Weigel G, et al. Comparison of different decellularization procedures of porcine heart valves. *Int J Artif Organs* 2003;26(5):421–427. [PubMed: 12828309]
14. Buinewicz B, Rosen B. Acellular cadaveric dermis (AlloDerm): a new alternative for abdominal hernia repair. *Ann Plast Surg* 2004;52(2):188–194. [PubMed: 14745271]
15. Chen RN, Ho HO, Tsai YT, Sheu MT. Process development of an acellular dermal matrix (ADM) for biomedical applications. *Biomaterials* 2004;25(13):2679–2686. [PubMed: 14751754]
16. Hudson TW, Liu SY, Schmidt CE. Engineering an improved acellular nerve graft via optimized chemical processing. *Tissue Eng* 2004;10(9–10):1346–1358. [PubMed: 15588395]
17. Hopper RA, Woodhouse K, Semple JL. Acellularization of human placenta with preservation of the basement membrane: a potential matrix for tissue engineering. *Ann Plast Surg* 2003;51(6):598–602. [PubMed: 14646657]
18. Mirsadraee S, Wilcox HE, Korossis SA, Kearney JN, Watterson KG, Fisher J, et al. Development and characterization of an acellular human pericardial matrix for tissue engineering. *Tissue Eng* 2006;12(4):763–773. [PubMed: 16674290]
19. Cartmell JS, Dunn MG. Effect of chemical treatments on tendon cellularity and mechanical properties. *J Biomed Mater Res* 2000;49(1):134–140. [PubMed: 10559756]
20. Grauss RW, Hazekamp MG, Oppenhuizen F, van Munsteren CJ, Gittenberger-de Groot AC, DeRuiter MC. Histological evaluation of decellularised porcine aortic valves: matrix changes due to different decellularisation methods. *Eur J Cardiothorac Surg* 2005;27(4):566–571. [PubMed: 15784352]
21. Lin P, Chan WC, Badylak SF, Bhatia SN. Assessing porcine liver-derived biomatrix for hepatic tissue engineering. *Tissue Eng* 2004;10(7–8):1046–1053. [PubMed: 15363162]
22. Woods T, Gratzner PF. Effectiveness of three extraction techniques in the development of a decellularized bone-anterior cruciate ligament-bone graft. *Biomaterials* 2005;26(35):7339–7349. [PubMed: 16023194]
23. Probst M, Dahiya R, Carrier S, Tanagho EA. Reproduction of functional smooth muscle tissue and partial bladder replacement. *Br J Urol* 1997;79(4):505–515. [PubMed: 9126077]
24. Yoo JJ, Meng J, Oberpenning F, Atala A. Bladder augmentation using allogenic bladder submucosa seeded with cells. *Urology* 1998 Feb 1;51(2):221–225. [PubMed: 9495701]

25. Bader A, Schilling T, Teebken OE, Brandes G, Herden T, Steinhoff G, et al. Tissue engineering of heart valves – human endothelial cell seeding of detergent acellularized porcine valves. *Eur J Cardiothorac Surg* 1998;14(3):279–284. [PubMed: 9761438]
26. McFetridge PS, Daniel JW, Bodamyali T, Horrocks M, Chaudhuri JB. Preparation of porcine carotid arteries for vascular tissue engineering applications. *J Biomed Mater Res A* 2004;70(2):224–234. [PubMed: 15227667]
27. Gulati AK. Evaluation of acellular and cellular nerve grafts in repair of rat peripheral nerve. *J Neurosurg* 1988;68(1):117–123. [PubMed: 3335896]
28. Jackson DW, Grood ES, Arnoczky SP, Butler DL, Simon TM. Freeze dried anterior cruciate ligament allografts. Preliminary studies in a goat model. *Am J Sports Med* 1987;15(4):295–303. [PubMed: 3661808]
29. Aimoli CG, Nogueira GM, Nascimento LS, Baceti A, Leirner AA, Maizato MJ, et al. Lyophilized bovine pericardium treated with a phenethylamine-diep-oxide as an alternative to preventing calcification of cardiovascular bioprosthesis: preliminary calcification results. *Artif Organs* 2007;31(4):278–283. [PubMed: 17437496]
30. Laun A, Tonn JC, Jerusalem C. Comparative study of lyophilized human dura mater and lyophilized bovine pericardium as dural substitutes in neurosurgery. *Acta Neurochir (Wien)* 1990;107(1–2):16–21. [PubMed: 2096603]
31. El-Sabban ME, El-Khoury H, Hamdan-Khalil R, Sindet-Pedersen S, Bazarbachi A. Xenogenic bone matrix extracts induce osteoblastic differentiation of human bone marrow-derived mesenchymal stem cells. *Regen Med* 2007;2(4):383–390. [PubMed: 17635046]
32. Ahn JI, Lee DH, Ryu YH, Jang IK, Yoon MY, Shin YH, et al. Reconstruction of rabbit corneal epithelium on lyophilized amniotic membrane using the tilting dynamic culture method. *Artif Organs* 2007;31(9):711–721. [PubMed: 17725699]
33. Ide C. Nerve regeneration and Schwann cell basal lamina: observations of the long-term regeneration. *Arch Histol Jpn* 1983;46(2):243–257. [PubMed: 6882155]
34. Lewis PB, Williams JM, Hallab N, Viridi A, Yanke A, Cole BJ. Multiple freeze-thaw cycled meniscal allograft tissue: a biomechanical, biochemical, and histologic analysis. *J Orthop Res* 2008;26(1):49–55. [PubMed: 17676620]
35. Zaleske D, Peretti G, Allemann F, Strongin D, MacLean R, Yates KE, et al. Engineering a joint: a chimeric construct with bovine chondrocytes in a devitalized chick knee. *Tissue Eng* 2003;9(5):949–956. [PubMed: 14633379]
36. Bullard KM, Banda MJ, Arbeit JM, Bergsland E, Young DM. Human acellular dermal matrix as a novel model of malignant epithelial cell invasion. *Invasion Metastasis* 1997;17(1):42–52. [PubMed: 9425323]
37. Coucouvanis E, Martin GR. Signals for death and survival: a two-step mechanism for cavitation in the vertebrate embryo. *Cell* 1995;83(2):279–287. [PubMed: 7585945]
38. Doetschman TC, Eistetter H, Katz M, Schmidt W, Kemler R. The in vitro development of blastocyst-derived embryonic stem cell lines: formation of visceral yolk sac, blood islands and myocardium. *J Embryol Exp Morphol* 1985;87:27–45. [PubMed: 3897439]
39. Itskovitz-Eldor J, Schuldiner M, Karsenti D, Eden A, Yanuka O, Amit M, et al. Differentiation of human embryonic stem cells into embryoid bodies compromising the three embryonic germ layers. *Mol Med* 2000;6(2):88–95. [PubMed: 10859025]
40. Keller GM. In vitro differentiation of embryonic stem cells. *Curr Opin Cell Biol* 1995;7(6):862–869. [PubMed: 8608017]
41. Nair R, Ngangan AV, McDevitt TC. Efficacy of solvent extraction methods for acellularization of embryoid bodies. *J Biomater Sci Polym Ed* 2008;19(6):801–819. [PubMed: 18534098]
42. Nair R, Shukla S, McDevitt TC. Acellular matrices derived from differentiating embryonic stem cells. *J Biomed Mater Res A* 2008;87(4):1075–1085. [PubMed: 18260134]
43. Carpenedo RL, Sargent CY, McDevitt TC. Rotary suspension culture enhances the efficiency, yield, and homogeneity of embryoid body differentiation. *Stem Cells* 2007;25(9):2224–2234. [PubMed: 17585171]

44. Guo Y, Graham-Evans B, Broxmeyer HE. Murine embryonic stem cells secrete cytokines/growth modulators that enhance cell survival/anti-apoptosis and stimulate colony formation of murine hematopoietic progenitor cells. *Stem Cells* 2006;24(4):850–856. [PubMed: 16339641]
45. Singla DK, McDonald DE. Factors released from embryonic stem cells inhibit apoptosis of H9c2 cells. *Am J Physiol Heart Circ Physiol* 2007;293(3):H1590–H1595. [PubMed: 17545477]
46. Singla DK, Singla RD, McDonald DE. Factors released from embryonic stem cells inhibit apoptosis in H9c2 cells through PI3K/Akt but not ERK pathway. *Am J Physiol Heart Circ Physiol* 2008;295(2):H907–H913. [PubMed: 18552162]

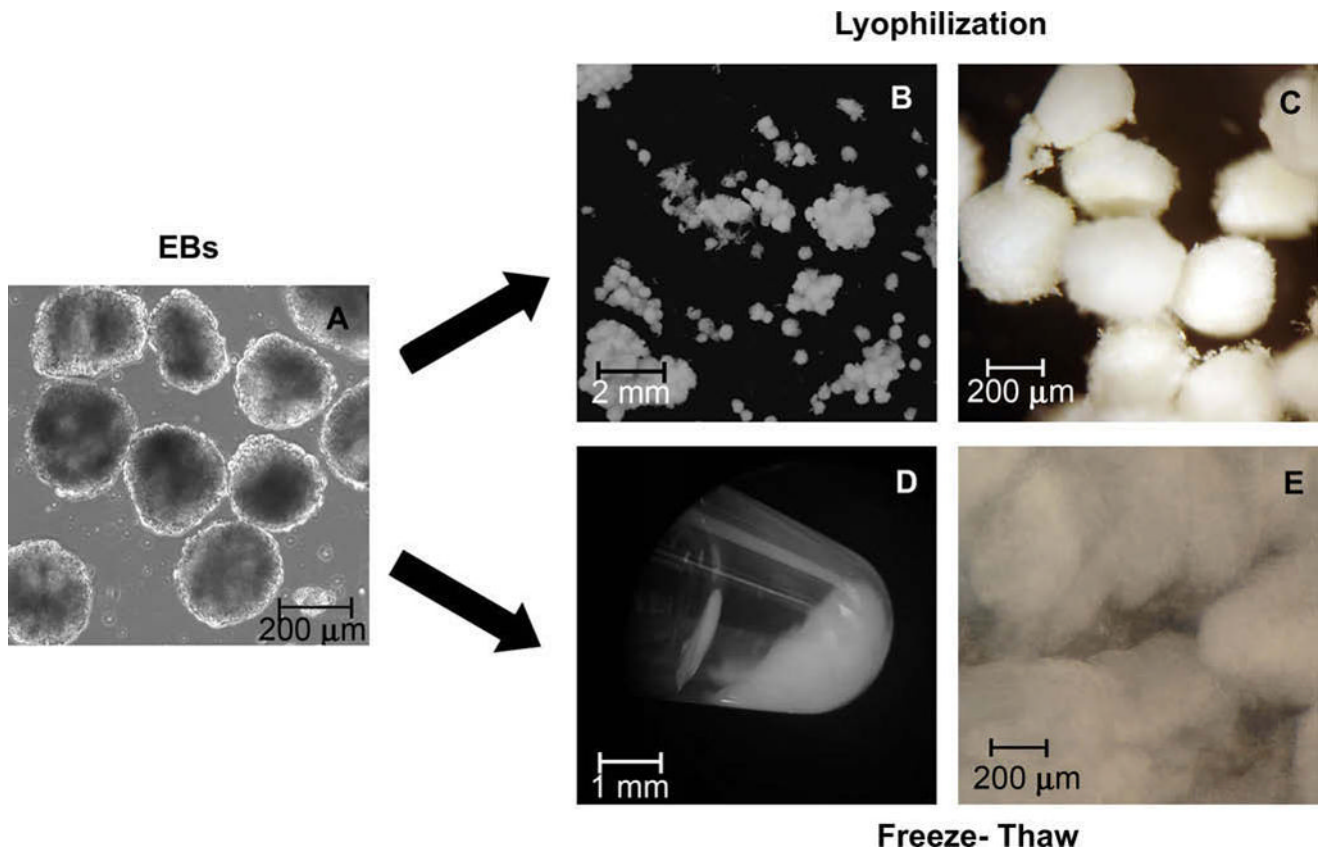


Fig. 1. Overview of EB acellularization process. EBs differentiated for 7 days were mechanically acellularized either by lyophilization (B and C) or multiple freeze-thaw cycles (D and E) followed by DNase treatment. Phase image shows EBs cultured for 7 days (A). Digital images macroscopically exhibit EB matrix following each of the mechanical acellularization techniques (B and D), including a closer image on the far right (C and E). Freeze-thaw matrix is shown as a pellet inside a microcentrifuge tube (D), while all other images (A–C, E) are presented within a Petri dish.

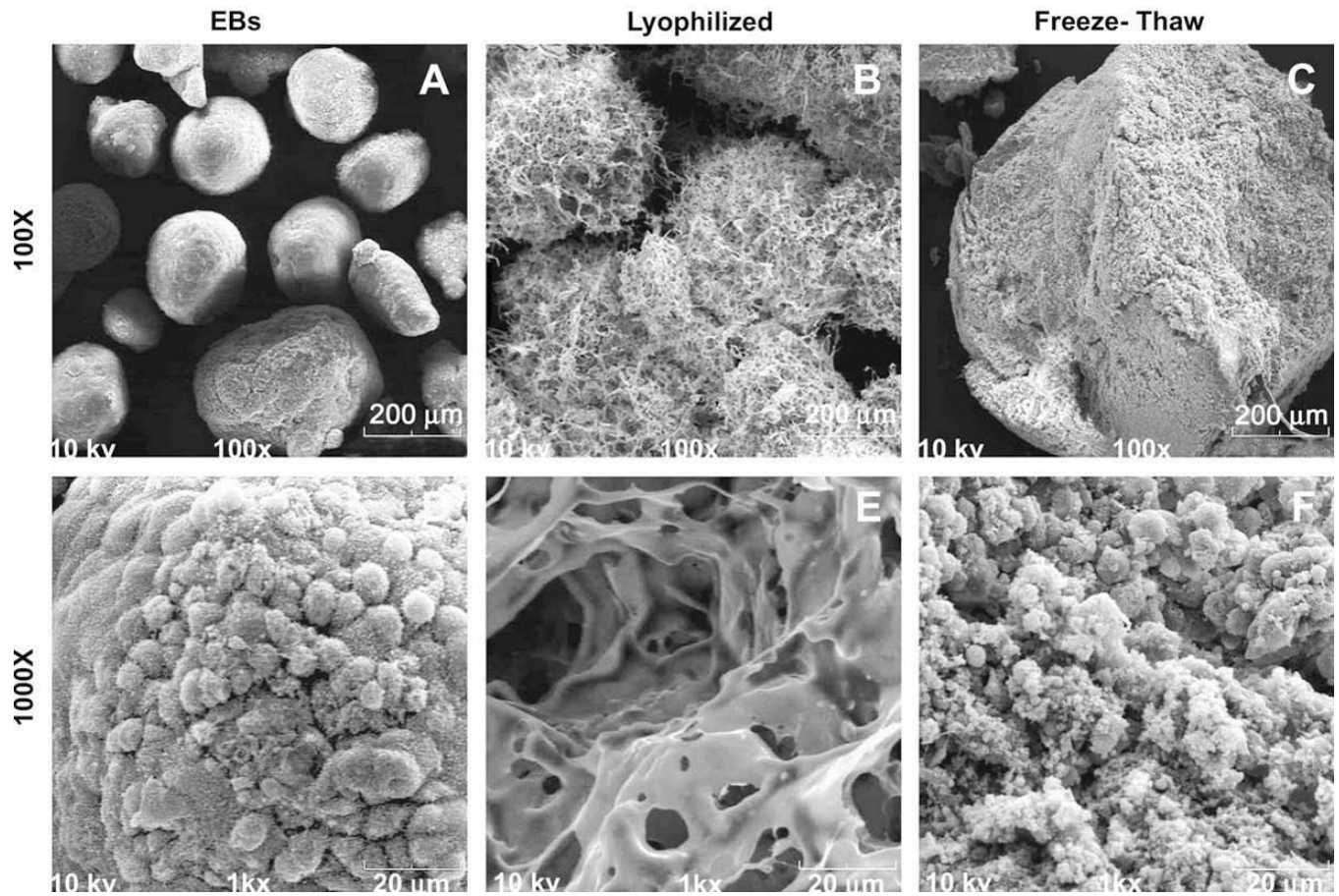


Fig. 2. Sample SEM images were taken before and after mechanical permeabilization at 100× (scale bar = 200 μm) and 1000× (scale bar = 20 μm) magnification. EBs (A and D) and lyophilized EBs (B and E) retain separate EB structure; however, lyophilized EBs show a more apparent porous structure compared to untreated EBs. Freeze-thawed EBs (C and F) no longer retained EB morphology and appeared to have a compact and dense structure.

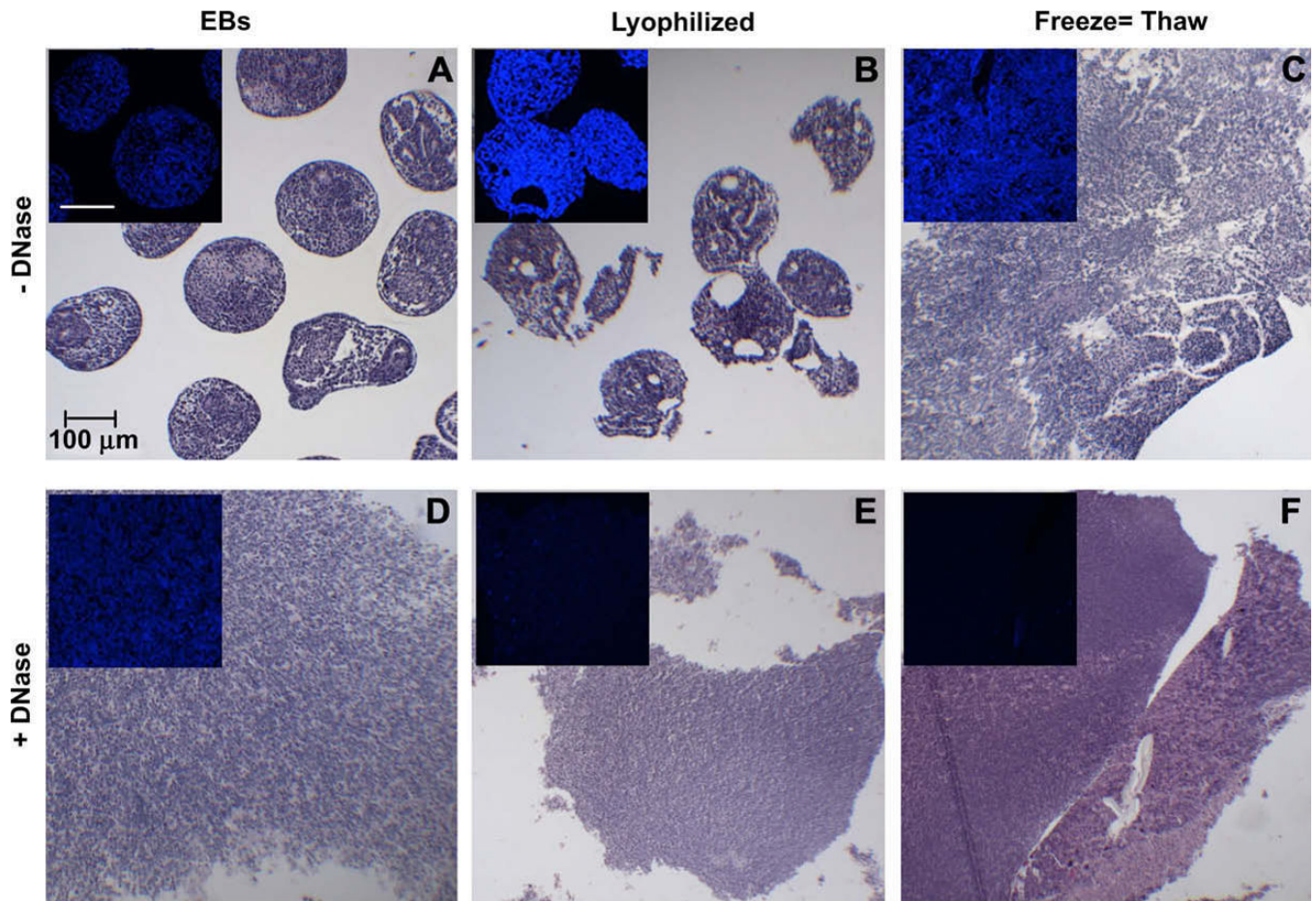
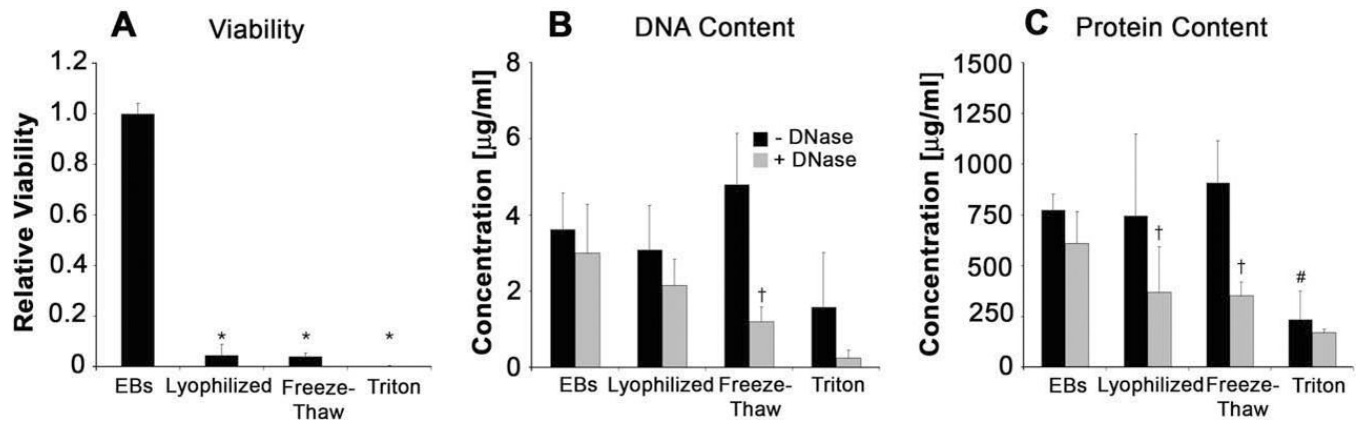


Fig. 3. Histological analysis of mechanical acellularization. EBs and acellular samples were stained with H&E and Hoechst (inset) to qualitatively compare acellular treatments. Mechanical disruption alone (top row, A–C) was compared to mechanical disruption and DNase treatment (bottom row, D–F). Scale bar = 100 μ m for each panel.

**Fig. 4.**

Quantitative analysis of acellular EB matrix components. (A) Relative cell viability of permeabilized samples. (B) Residual DNA concentration pre- and post-DNase treatment. FT permeabilization lead to significant removal of DNA following treatment with DNase. (C) Total protein content pre- and post-DNase treatment. Total protein before DNase treatment in Triton samples was significantly lower than all other treatments; whereas post-DNase treatment of mechanically permeabilized samples significantly decreased protein content compared to no DNase treatment. One-way ANOVA ($p < 0.05$): * significant compared to untreated EBs. Two-way ANOVA ($p < 0.05$): # significant compared to other DNase treatment samples, †significant compared to same permeabilization, +DNase samples. Results shown are mean \pm standard deviation based on 2×10^3 EBs per sample.

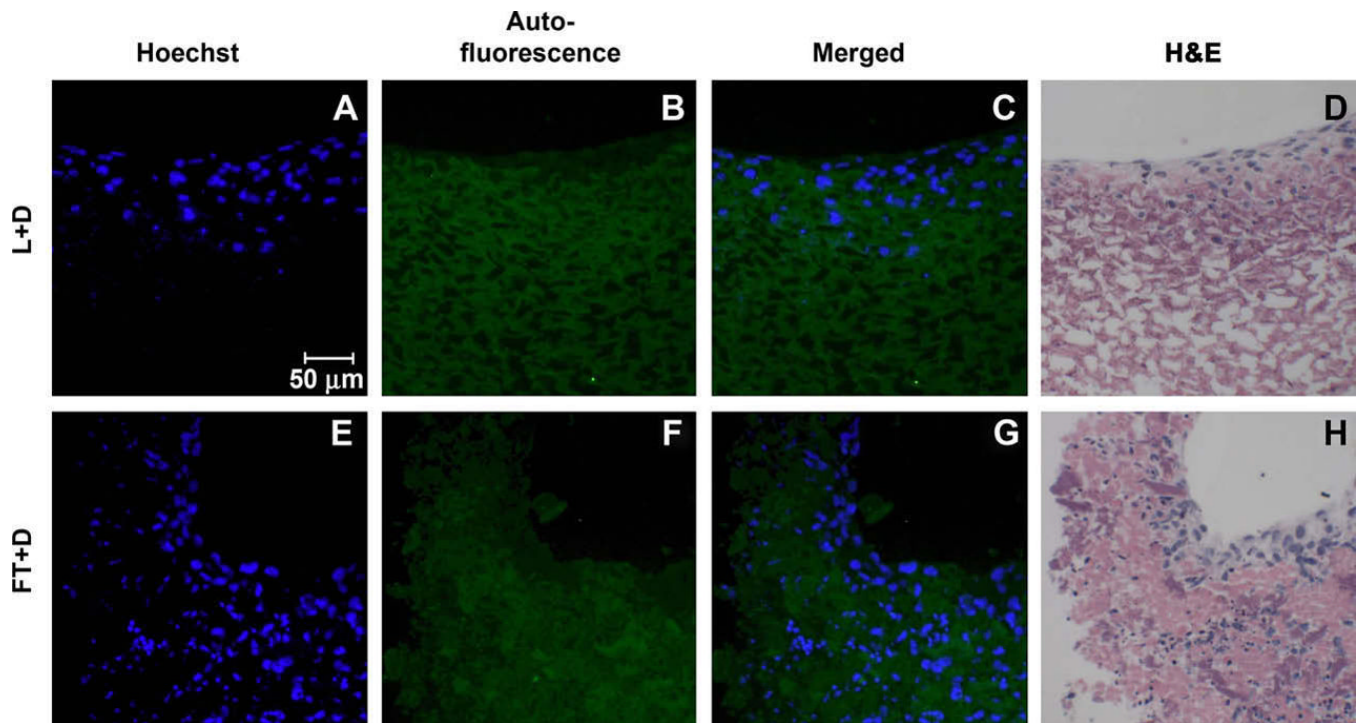


Fig. 5. Cell attachment to acellular EB matrices was assessed by seeding NIH-3T3 fibroblasts onto the materials. Fibroblasts were stained with Hoechst (blue; A and E), while the acellular matrix was visualized via auto-fluorescence (FITC channel; B and F). Additionally, seeded matrices were stained with H&E to demonstrate successful repopulation (D and H). Exogenous cells attached and repopulated both the L + D matrix (A–D) and the FT + D matrix (E–H).